

Supporting Information

Designing Locally Ordered Structures of MnO₂ for High-Rate Cathode in Aqueous Zinc-Ion Batteries

Shuhao Zhou^{a, b}, Shengyu Liang^b, Shanshan Liu^b, Shouyue Wang^b, Wei Zhang^b, Meng Li^c, Jingxia Qiu^{*a}, Sheng Li^{*b}

^a School of Physical and Mathematical Sciences, Nanjing Tech University (NanjingTech), Nanjing 211816, China

^b Key Laboratory of Flexible Electronics (KLOFE) and Institute of Advanced Materials (IAM), School of Flexible Electronics (Future Technologies), Nanjing Tech University (NanjingTech), Nanjing 211816, China

^c Institute for Sustainable Transformation, School of Chemical Engineering and Light Industry, Guangdong University of Technology, Guangzhou Mega University Town, Guangzhou 510006, China

EXPERIMENTAL SECTION

Materials Preparation

Firstly, 3.16 g KMnO_4 and 4.56 g $\text{H}_2\text{C}_2\text{O}_4$ are dissolved in 500 mL deionized water (DI water) and vigorously stirred. Then, the KMnO_4 solution was added to the $\text{H}_2\text{C}_2\text{O}_4$ solution dropwise and reacted for 8 hours under vigorous stirring in an ambient atmosphere. After that, the precipitate was collected by centrifugation and washing with DI water three times, followed by a freeze-drying process. At last, the final product (LOM) was obtained by annealing the precipitate in an air atmosphere for 9 hours at 300 °C with a heating rate of 5 °C/min.

The synthesis method of $\alpha\text{-MnO}_2$ is derived from the previous report¹. Firstly, 0.507 g $\text{MnSO}_4\cdot\text{H}_2\text{O}$ and 2 mL 0.5 mol L^{-1} H_2SO_4 were dissolved in 60 mL DI water and vigorously stirred for 10 min. Then, 0.316 g KMnO_4 was dissolved in 20 mL DI water and added to the $\text{MnSO}_4\cdot\text{H}_2\text{O}$ solution dropwise, followed by vigorously stirring for one hour in an ambient atmosphere. After that, the mixture was ultrasonicated for 30 min before being sealed into a 100 mL Teflon-lined autoclave for 12 h at 120 °C. Finally, the product ($\alpha\text{-MnO}_2$) was collected by centrifugation and washing with DI water three times, followed by air drying.

Preparation of the LOM Electrode.

Mixing LOM, Super-P, MWCNT, and PVDF in the NMP solvent with a weight ratio of 7:1:1:1 to form a slurry. MWCNT was added to construct a conductive network without changing the whole weight ratio of the conducting component. Then, the slurry was spread on the Ti foil current collector and kept heating at 60 °C in the air drying oven overnight. At last, the electrode was made by cutting the Ti foil loading with slurry into discs with a diameter of 14 mm. The average mass loading of the electrode ranges from 0.8-1.2 mg.

Preparation of the α -MnO₂ Electrode and Battery Assembling.

The process is the same as the LOM electrode, except that the slurry was formed with α -MnO₂, Super-P, MWCNT, and PVDF in the NMP solvent with a weight ratio of 7:1:1:1. Pure zinc foil was cut into discs with a diameter of 14 mm and used as the anode. Glass fiber (GF/F) was used as a separator. An aqueous electrolyte consisted of 2 M ZnSO₄ + 0.25 M MnSO₄. MnSO₄ was added to the electrolyte to restrain the dissolution of Mn²⁺. The coin-type (CR2025) battery was assembled using materials prepared above in an ambient atmosphere.

Material Characterization and Electrochemical Measurements.

Material Characterization. The morphology and microstructure of electrode materials are investigated by scanning electron microscopy (JEOL, JSM-7800F) and transmission electron microscopy ((JEOL, JEM-2100F). Element distribution of LOM is detected by EDS Mapping. The detailed nanostructure of LOM is characterized by high-resolution transmission electron microscopy (HRTEM). Selected area electron diffraction (SAED) and X-ray diffraction (XRD, Rigaku, Smartlab, Cu K α radiation, λ = 1.5418 Å) were introduced to confirm the structure properties of electrode materials. The chemical valence state is analyzed using X-ray photoelectron spectroscopy (XPS, Thermo Fisher, ESCALAB250Xi). The existence of oxygen vacancies and variation of the structure is confirmed by electron paramagnetic resonance (EPR, Bruker, EMXplus-6/1) spectroscopy and laser confocal Raman microscope (Raman, Witec, Alpha300).

Electrochemical Measurements. The galvanostatic charge-discharge tests of the CR2025 coin-type battery were performed on a battery test system (LAND, CT-2001A) with an operating voltage of 1-1.85 V. Cyclic voltammetry (CV) test was conducted on an electrochemical workstation (Bio-logic, VMP-300). Electrochemical impedance

spectroscopy (EIS) tests were measured using CORRTEST CS3104.

Computational Details.

All the calculations are performed in the framework of the density functional theory with the projector augmented plane-wave method, as implemented in the Vienna ab initio simulation package². The generalized gradient approximation proposed by Perdew, Burke, and Ernzerhof is selected for the exchange-correlation potential³. The long-range van der Waals interaction is described by the DFT-D3 approach⁴. The cut-off energy for the plane wave is set to 520 eV. DFT+U corrections are introduced with $U=3.9$ eV (according to the Materials project) to describe the strong on-site Coulomb interaction of localized *d*-electrons of Mn. The energy criterion is set to 10^{-6} eV in the iterative solution of the Kohn-Sham equation. The Brillouin zone integration is performed using a $2 \times 2 \times 1$ k-mesh. The mixture of the LOM model was obtained by an AIMD heating at 4000 K with half of the atoms fixed. Before DOS calculations, all the structures are relaxed until the residual forces on the atoms have declined to less than 0.03 eV/Å.

1. B. Wu, G. Zhang, M. Yan, T. Xiong, P. He, L. He, X. Xu and L. Mai, *Small*, 2018, **14**, 1703850.
2. G. Kresse and D. Joubert, *Phys. Rev. B.*, 1999, **59**, 1758-1775.
3. J. P. Perdew, K. Burke and M. Ernzerhof, *Phys. Rev. Lett.*, 1996, **77**, 3865-3868.
4. S. Grimme, J. Antony, S. Ehrlich and H. Krieg, *J. Chem. Phys.*, 2010, **132**.

Supplementary Figures

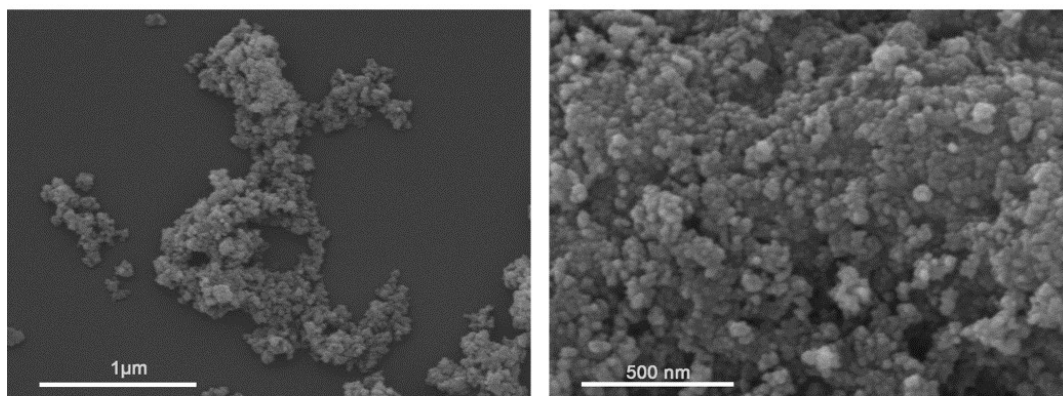


Figure S1. SEM images of LOM.

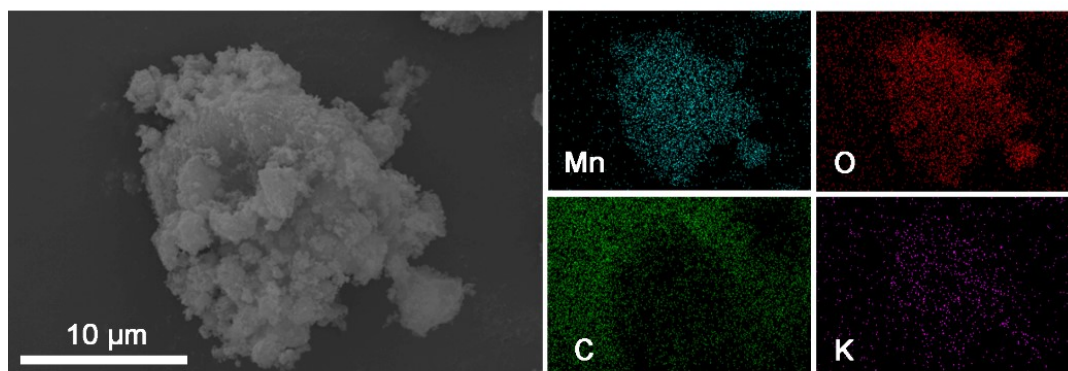


Figure S2. EDS mapping of Mn, O, C, and K elements.

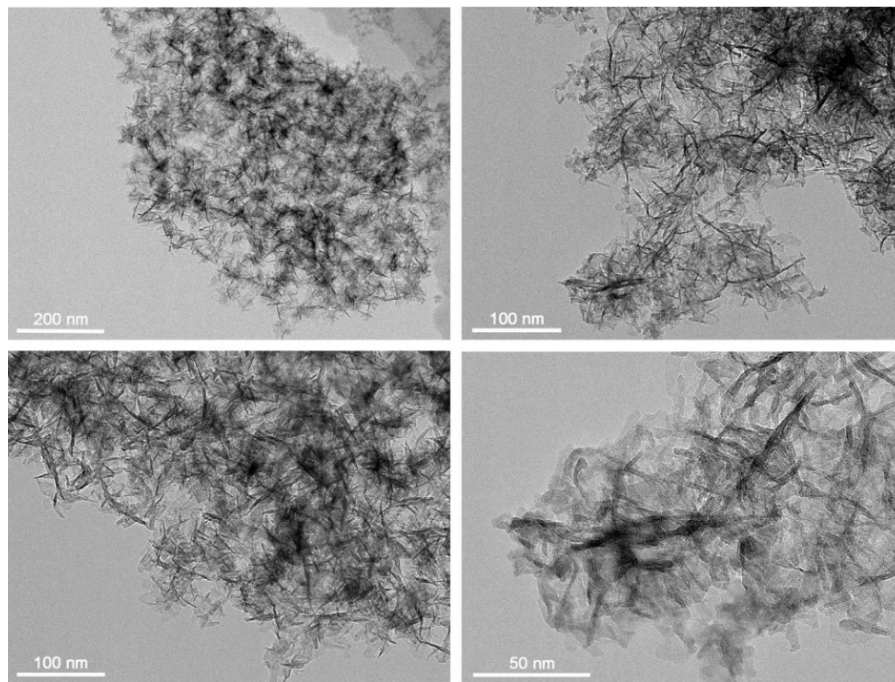


Figure S3. TEM images of LOM.

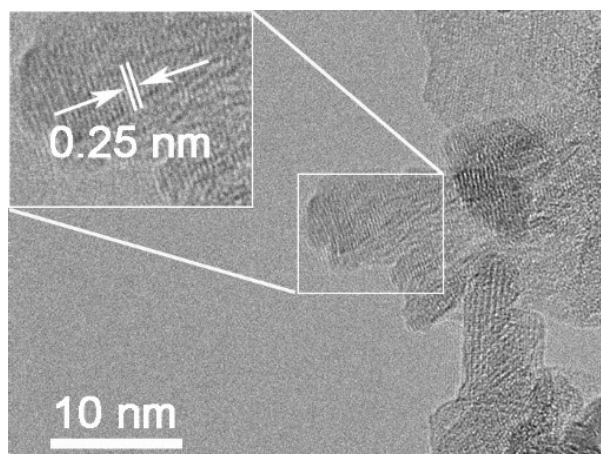


Figure S4. HRTEM image of LOM.

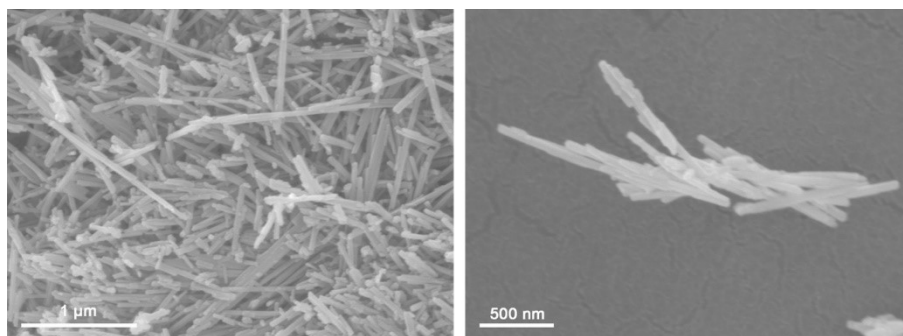


Figure S5. SEM images of α - MnO_2 .

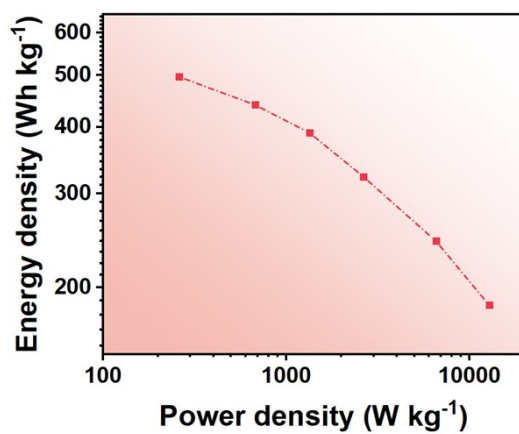


Figure S6 The Ragone plot of the LOM electrode.

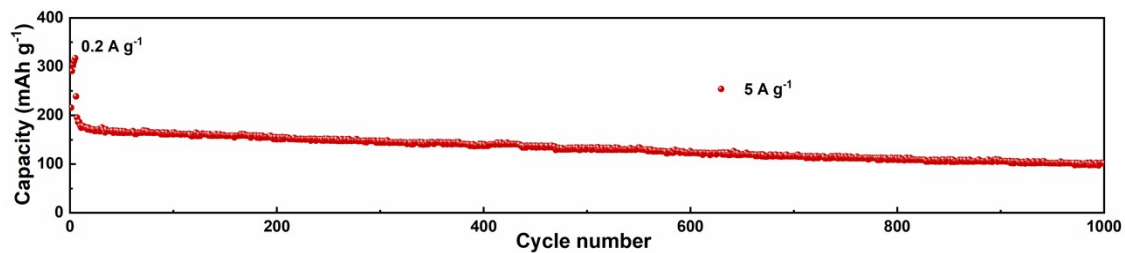


Figure S7. Long cycling performance of the LOM electrode at 5 A g⁻¹.

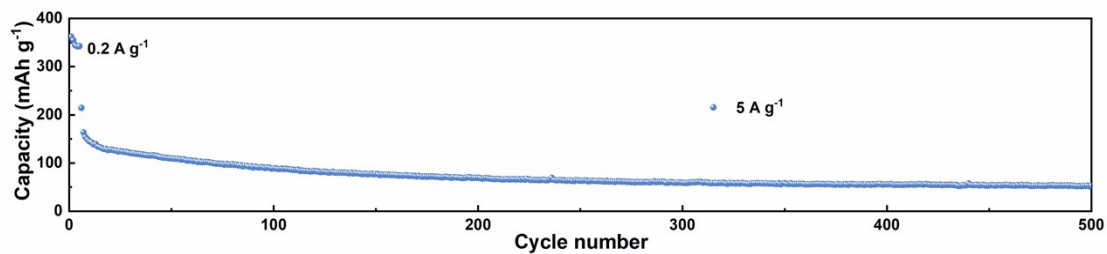


Figure S8. Long cycling performance of the α -MnO₂ electrode at 5 A g⁻¹.